J. Mol. Model. **1998**, *4*, 73 – 82

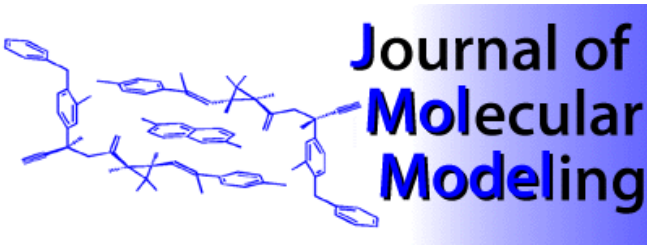

FULL PAPER

Conformation of the Flavin Adenine Dinucleotide Cofactor FAD in DNA-Photolyase: A Molecular Dynamics Study

Jutta Hahn, Maria-Elisabeth Michel-Beyerle, and Notker Rösch

Institut für Physikalische und Theoretische Chemie, Technische Universität München, D-85747 Garching, Germany.
E-mail: roesch@theochem.tu-muenchen.de

Received: 10 December 1997 / Accepted: 3 February 1998 / Published: 16 February 1998

Abstract In order to gain insight into the light-driven repair of DNA by the enzyme DNA photolyase, the conformation of the photoactive cofactor FAD, a flavin adenine dinucleotide, has been studied by molecular dynamic simulations. In contrast to FAD in the gas phase and in water where the MD procedure yields various "open" I-shaped as well as "closed" U-shaped conformations, the calculations of FAD binding to the enzyme show essentially a single U-shaped conformation of this cofactor which, so far, is unique among FAD-carrying proteins. It is characteristic for this U-shaped conformation that the FAD components occupy opposite sides of the pocket in the surface of the protein which provides the binding site for the defect pyrimidine dimer structure on DNA. In fact, the calculated U-shaped conformation is very close to the one revealed by the X-ray structure analysis of DNA photolyase. Moreover, the simulations yield details on the binding of the photoactive isoalloxazine moiety and the dynamics of the amino acids forming the binding cavity of the enzyme.

Keywords FAD, Photolyase, Molecular dynamics

Introduction

It is well established that the enzyme photolyase repairs UV induced damage to DNA by splitting the ring of the predominant photoproduct, the cis,syn-cyclobutane pyrimidine dimer, into the corresponding pyrimidine monomers [1-3]. The photoactive components of this enzyme are the reduced flavin adenine dinucleotide, $FADH^-$, and 5,10–methenyltetrahydrofolylpolyglutamate (MTHF). Thus far, the crudely understood sequence of events during the repair process involves the following steps: (i) recognition of the DNA defect by photolyase and its structure-specific binding, (ii) excitation of the photoactive cofactor $FADH^-$, either directly or via excitation energy transfer from MTHF, (iii) electron transfer from the excited $FADH^-$ to the pyrimidine dimer, (iv) splitting of the cyclobutane ring in the dimer and back transfer of the electron and finally (v) desorption of the enzyme from the repaired DNA substrate. A dimer splitting scheme based on quantum chemical calculations of the activation energies indicates that first the C5–C5' bond and then the C6–C6' bond is broken [4], a result which is still open to experimental confirmation.

As revealed in the crystal structure analysis [1], a pocket in the enzyme allows optimal access of the dimer substrate

Correspondence to: N. Rösch

to the cofactor FAD involved in the repair process and thus is likely to be the binding site for the DNA defect. A striking feature of the crystal structure analysis is the U-shaped conformation of FAD [1]. The FAD molecule consists of the photoactive component isoalloxazine and the groups ribose, phosphate and adenosine (see Figure 1). The FAD molecule in the enzyme is bent in such a way that the isoalloxazine and adenosine moieties are facing each other. This conformation of the photolyase cofactor FAD seems to be unique as it differs fundamentally from "classical" binding conformations studied so far which show FAD in an elongated, I-shaped structure [a]. This difference in binding conformation may reflect the diversity of the functions of FAD cofactors [1].

The present work aims at elucidating this apparent conformational uniqueness of FAD in the photolyase enzyme by molecular dynamic (MD) calculations. We investigated both $FADH^-$, which is the active form in the repair process, and $FADH_2$, the fully reduced species. Whenever both species behave in the same fashion, we shall use the generic term FAD. In order to broaden the basis of the discussion also the environment of the chromophore was taken into account: FAD has been studied in the gas phase, in aqueous solution, and in the protein matrix provided by the enzyme photolyase as obtained from the crystal structure [1]. In the latter case, the dynamics of the amino acids as well as of water molecules inside the binding cavity of the enzyme was investigated, both for the crystal water as well as for additional water molecules at random positions. In addition, partial charges and the ionization potential of FAD were determined in semi-empirical quantum chemical calculations.

Computational Details

All force field calculations, geometry optimizations as well as MD simulations, were based on the AMBER force field [27,28] as provided by the program DISCOVER [29]. The crystal structure of the DNA photolyase including the cofactors and crystal water molecules were chosen as starting geometry (Protein Data Bank entry: 1dnp) [1]. In order to take solvent effects into account a sphere of 20 Å radius, centered at the entrance of the pocket of the photolyase enzyme, was filled with additional 516 water molecules. In this way, the pocket is filled and the surface of the enzyme in the vicinity of the pocket is solvated. The water molecules and the protein are allowed to freely move during the simulation. An analogous approach was taken to simulate the flavin molecule in aqueous solution; 585 water molecules were arranged in a sphere of 20 Å radius around the flavin.

The potential types for the photolyase enzyme and the water molecules are chosen in standard fashion [27–29]; the charges of glutamic and aspartic acid are negative while arginine and lysine are positively charged. For $FADH^-$, the potential types are assigned in the following manner; first the atom labels as designated in Figure 1 and then the potential types are given, following AMBER conventions: PF1/P, OF2/O2, OF3/O2, OF4/OS, O/OS, C/CT, HC1/HC, HC2/HC, C1/CT, H1/HC, O1/OH, HO1/HO, C2/CT, H2/HC, O2/OH, HO2/HO, C3/CT, H3/HC, O3/OH, HO3/HO, C4/CT, H41/HC, H42/HC, N/NA, HN/H, N1/N*, N2/NA, (HN2/H), C5/CM, C6/C, O4/O, N3/N, HN3/H, C7/C, O5/O, C4A/CM, C5A/CA, C8/CA, H8/HC, C9/CA, C7M/CT, H7M1/HC, H7M2/HC, H7M3/HC, C10/CA, C8M/CT, H8M1/HC, H8M2/HC, H8M3/HC, C11/CA, H11/HC, C9A/CA, P/P, O1P/O2, O2P/O2, O6/OS, C12/CS, H12/HT, C13/CT, H131/HC, H132/HC, C14/CS, H14/HT, O7/OE, C15/CS, H15/HT, N4/N*, C16/CB, N5/NC, C17/CQ, H17/HC, N6/NC, C18/CA, N7/N2, H71/H2, H72/H2, C19/CB, N8/NB, C20/CK, H20/HC, C21/CS, H21/HT, O8/OT, HO8/HY, O9/OT, H9/HY. In case of $FADH_2$, the additional hydrogen is bound to the center N2.

The partial charges for the atomic centers of FAD as required by the AMBER force field were estimated by a quantum chemical calculations (from a Mulliken analysis) employing the semi-empirical method PM3 as provided by the program MOPAC, version 6.0 [30,31]. The PM3 method is known to be best suited for phosphorus containing compounds; however, checks with AM1 calculations yielded very similar charges. The calculated charges for both reduced forms, $FADH_2$ and $FADH^-$, differ mainly in the heterocycles of the isoalloxazine fragment; we list the partial charges (in au) for the atomic centers of this fragment, discriminating $FADH_2$ and $FADH^-$, respectively: N1 0.16/0.17, C5 –0.01/0.10, N2 0.06/–0.37, HN2 0.18/–, C6 0.18/0.24, O4 –0.39/-0.47, N3 0.12/0.09, HN3 0.12/0.08, C7 0.29/0.30, O5 –0.45/–0.56, C4A –0.38/–0.52, N 0.18/0.23, HN 0.10/0.08. In the following, the remaining values are listed; only the partial charges of $FADH_2$ shall be given where their difference between $FADH_2$ and $FADH^-$ is less than 0.02 au: PF1 2.15, OF2 –1.09, OF3 –0.99, OF4 –0.96, O –0.64, C 0.10, HC1 0.05, HC2 0.02, C1 0.04, H1 0.05, O1 –0.45, HO1 0.33, C2 0.01, H2 0.07, O2 –0.37/–0.30, HO2 0.26/0.21, C3 0.04, H3 0.05, O3 –0.38, HO3 0.27, C4 –0.10, H41 0.07/0.03, H42 0.08, C5A –0.02, C8 –0.20/–0.25, H8 0.11, C9 –0.04, C7M -0.06, H7M1 0.04, H7M2 0.04, H7M3 0.05, C10 -0.14/–0.18, C8M –0.05, H8M1 0.04, H8M2 0.03, H8M3 0.04, C11 -0.07/–0.11, H11 0.12, C9A –0.13, P 2.15, O1P –1.02, O2P –1.02, O6 –0.67, C12 0.01, H12 0.12, C13 0.14, H131 0.02, H132 0.05, C14 0.02, H14 0.04, O7 -0.26, C15 0.06, H15 0.09, N4 0.27, C16 –0.11, N5 –0.13, C17 0.03, H17 0.10, N6 –0.28, C18 0.06/0.09, N7 0.12, H71 0.10, H72 0.06, C19 –0.26, N8 –0.12, C20 –0.13, H20 0.21, C21 0.01, H21 0.09/0.12, O8 -0.35, HO8 0.23, O9 –0.40, H9 0.30. Each derivative of FAD was examined in I- and U-shaped conformation, but only in-

[a] The references to the proteins including the flavin cofactor are made by the Protein Data Bank tracking code numbers: 1buc [5], 1gal [6], 1ger [7], 1gra [8], 1grb [8], 1gre [8], 1grf [8], 1grg [8], 1ius [9], 1iut [9], 1iuu [9], 1lpf [10], 1lvl [11], 1nda [12], 1npx [13], 1pbe [14], 1phh [15], 1pxa [16], 1pxb [16], 1pxc [16], 1tde [17], 1tdf [17], 1trb [18], 1typ [19], 1tyt [20], 2npx [21], 2tpr [22], 3grs [23], 3lad [24], 3mdd [25], 3mde [25], 5fx2 [26].

significant differences in the partial charges were found; in most cases they amount to less than 0.04 au, only at the oxygen centers of the phosphate groups differences reach 0.06 au.

The MD simulations were performed using the program Discover, version 95.0 [29]. For nonbonded interactions, described by van der Waals forces, an atom-based cut-off at 9.5 Å was imposed. Long-range Coulomb interactions were evaluated with the cell multipole method [32–34]. Energy minimizations were performed until the absolute value of the largest derivative was below 0.01 kcal/mol/Å. Steepest descent and conjugated gradient (Polak-Ribiere scheme [35]) methods were used in most cases. Additionally, for FAD in the gas phase and in the water solvent the quasi-Newton-Raphson algorithm in combination with the BFGS update scheme was applied [35]. The MD runs were executed with time steps of 1 fs. In case of the free flavin molecule and for FAD in aqueous solution, each MD run was carried out up to 500 ps at a temperature of 800 K in order to explore the conformation space efficiently. During the first 100 ps the system was equilibrated, the remaining simulation time was used for 4 independent samplings of 100 ps each; every 5 ps the coordinates are saved. After the MD simulation each of the saved structures was used as starting geometry for a subsequent energy minimization. For the photolyase enzyme the MD run at a temperature of 300 K was performed up to 300 ps: 80 ps for equilibration and 11 independent samplings, 20 ps each.

The color rendering of the three-dimensional structures displayed in the figures was carried out with the help of the program Schakal, version 96 [36].

Results and Discussion

Calculations on FAD in the gas phase

The MD simulation with subsequent minimizations was carried out to explore the conformation space of FAD and to analyze possible structures of FAD. As expected, these simulations show a number of different conformations in an energy range of about 8 kcal/mol; the conformations can easily be converted into each other. Rather large standard deviations of up to 60° calculated for dihedral angles (see Table 1) are indicative for the overall flexibility of FAD. It is not possible to classify the resulting structures using dihedral angles or to identify a clear preference for one of the conformations. To illustrate the structural variations of FAD according to this MD simulation, consider the values of the N1–N4 distances; they range from 4 to 14 Å for $FADH_2$ and from 4 to 16 Å for $FADH^-$ (see Figure 1 for the atom labelling). No preferred distance or distance range was found. Moreover, the energy minimized U-shaped FAD crystal structure (Figure 2) is about 2 kcal/mol higher in energy than the lowest energy conformation which is of I-shaped form (see Figure 3).

A crude estimate on this energy difference was attempted with PM3 single point calculations for prototypical structures of FAD as optimized with the AMBER force field. These PM3 calculations showed the U-shaped structure of FAD to be about 10 kcal/mol more stable than the I-shaped structure. Furthermore, first ionization potentials were determined by applying Koopmans' theorem after the anionic phosphate groups of FAD had been neutralized by protons. No significant differences between the ionization potentials of U- and I-shaped FAD were found. Depending on the structure, the first ionization potential is calculated in a range of 3.6–4.1 eV for $FADH^-$ and 7.5–7.8 eV for $FADH_2$. However, the calculations on FAD in the gas phase (or employing a spherical reaction field cavity) are not suitable to reliably estimate differences of binding energy or ionization potentials for FAD in the specific electric field set up by a protein matrix.

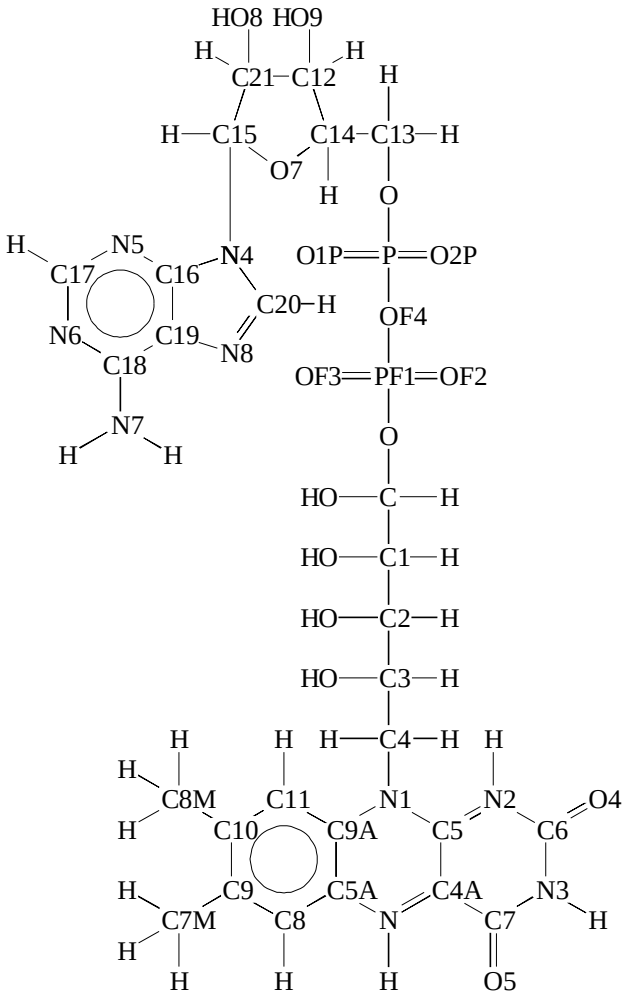

Figure 1 *Atom labeling scheme of $FADH_2$ showing the different components (from top to bottom): adenosine, phosphate, ribose, and isoalloxazine. In $FADH^-$, the hydrogen bound to center N2 is absent*

Table 1 *Comparison of Characteristic Structural Features of $FADH_2$ and $FADH^-$ for the Crystal Structure and for Conformations Determined with the AMBER Force Field*

Structural Parameters [a]				Crystal structure [b]	$FADH_2$ A [c]	$FADH_2$ B [d]	$FADH_2$ C [e]		$FADH^-$ A [c]	$FADH^-$ B [d]	$FADH^-$ C [e]	
C9A	N1	C4	C3	94	86	82	93	(8)	44	60	92	(7)
N1	C4	C3	C2	110	51	52	64	(9)	161	132	81	(9)
C4	C3	C2	C1	155	172	176	174	(5)	169	169	175	(4)
C3	C2	C1	C	148	178	164	85	(12)	180	179	86	(10)
C2	C1	C	O	178	153	165	171	(7)	169	178	170	(7)
C1	C	O	PF1	167	162	164	159	(11)	155	146	162	(9)
C	O	PF1	OF4	39	93	137	42	(12)	79	74	52	(15)
O	PF1	OF4	P	159	47	28	75	(13)	55	61	58	(25)
PF1	OF4	P	O6	137	52	62	159	(12)	158	164	130	(39)
OF4	P	O6	C13	94	64	60	66	(12)	56	56	65	(12)
P	O6	C13	C14	135	168	157	125	(11)	122	119	144	(21)
O6	C13	C14	C12	58	57	51	55	(13)	61	61	57	(12)
C21	C15	N4	C20	86	104	116	96	(13)	83	74	101	(14)
N1	N4			5.9	6.9	6.5	6.0	(0.4)	8.1	7.8	6.1	(0.5)
α				3	8	3	7	(5)	28	10	7	(4)

[a] Selected dihedral angles (in degrees) of the FAD backbone, distance N1-N4 (in Å) and interplanar angle α of the isoalloxazine moiety (in degrees; see text for the definition)
[b] Ref. 1
[c] U-shaped geometry determined by energy minimization starting with the enzyme crystal structure
[d] U-shaped geometry of the energy minimized structure of FAD in aqueous solvent
[e] Mean values and standard deviations (in parentheses) of the FAD geometry as obtained in the MD simulation of the enzyme.

In order to clarify the uniqueness of the U-shaped conformation of FAD in the photolyase enzyme,[1] 32 experimentally determined structures of the coenzyme FAD, which are available through the Protein Data Bank (PDB), were analyzed [5–26]. Only more or less I-shaped conformations were found, exhibiting a N1–N4 distance range of about 13–16 Å. Most of these molecules are incorporated in enzymes in such a way that either the adenine or the isoalloxazine moiety is bound to the enzyme while the other subunit juts out. For such arrangements the I-shaped conformation, featuring a larger N1–N4 distance, is the most evident one. For comparison we mention that for U-shaped conformations this distance takes a value of about 6 Å, in the photolyase crystal structure [1] as well as in the MD simulations of the enzyme (see Table 1).

It is interesting to note that the U-shaped form of FAD as realized in the photolyase enzyme was found among the local minima structures identified in our combined MD/minimization procedure. Therefore, we studied this structure in more detail. The energy minimization of free U-shaped FAD leads to a somewhat relaxed geometry (see Table 1). Although the adenine and isoalloxazine moities are slightly further apart

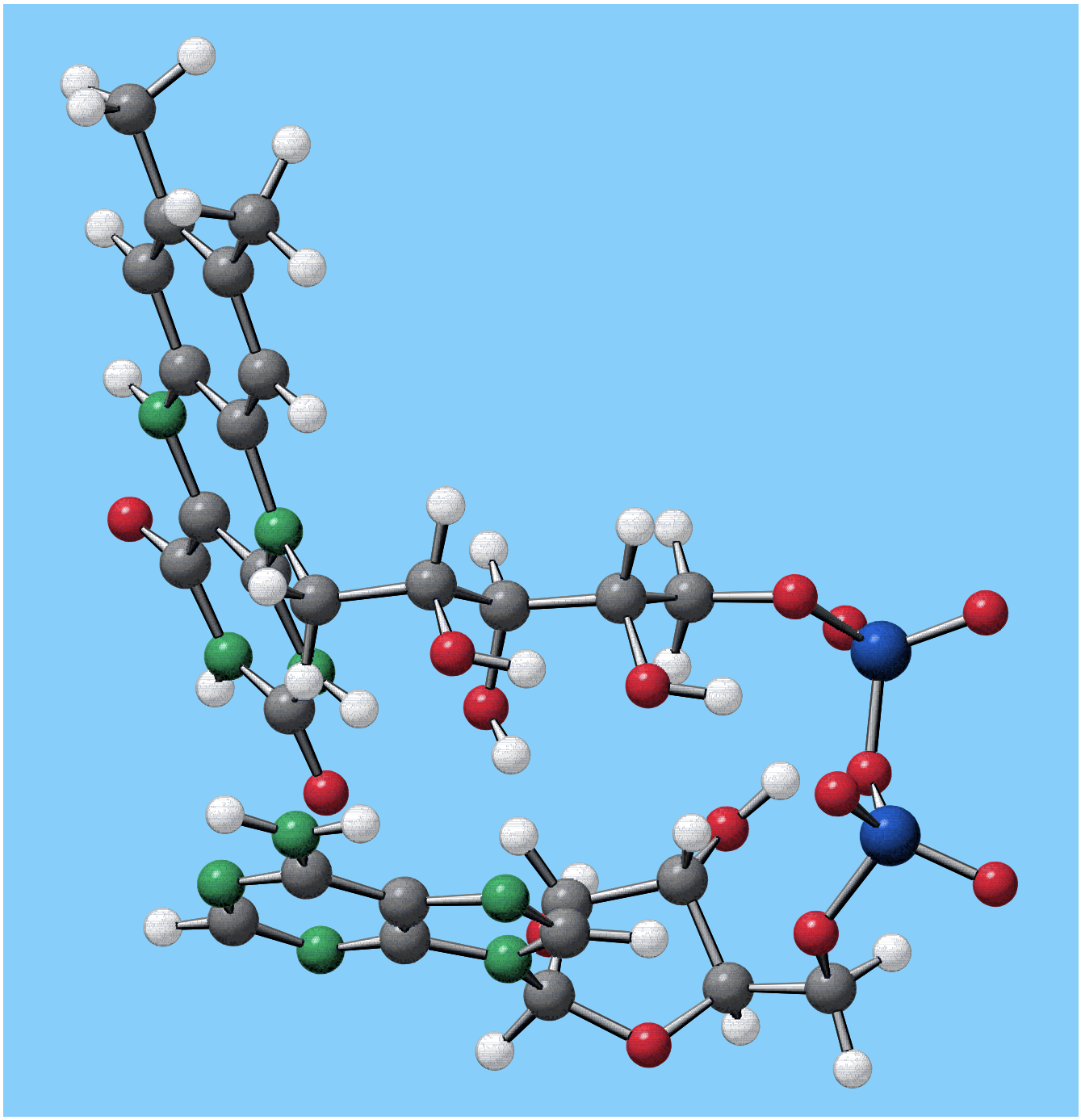

Figure 2 *U-shaped structure of $FADH_2$ as minimized with the AMBER force field. This conformation is similar to the crystal structure shown in Figure 4*

from each other than in the crystal structure, as measured by the increase of the N1–N4 distance (by 1.0–2.2 Å, see Table 1), the overall conformation remains U-shaped (see Figure 2) and both FAD derivatives will still fit well into the pocket of the photolyase enzyme. The calculated dihedral angles of the FAD backbone atoms differ by up to about 110° compared to the crystal structure (Table 1). Although torsions around the P–O bonds are known to be quite flexible, the fold formed by the phosphate groups exhibits a similar shape as in the crystal structure. Dihedral angles involving C–C bonds tend to be trans (180°) or gauche (60°) as one can clearly see in the relaxation of the dihedral angle N1–C4–C3–C2 (Table 1). In the crystal structure, the angle is 110°

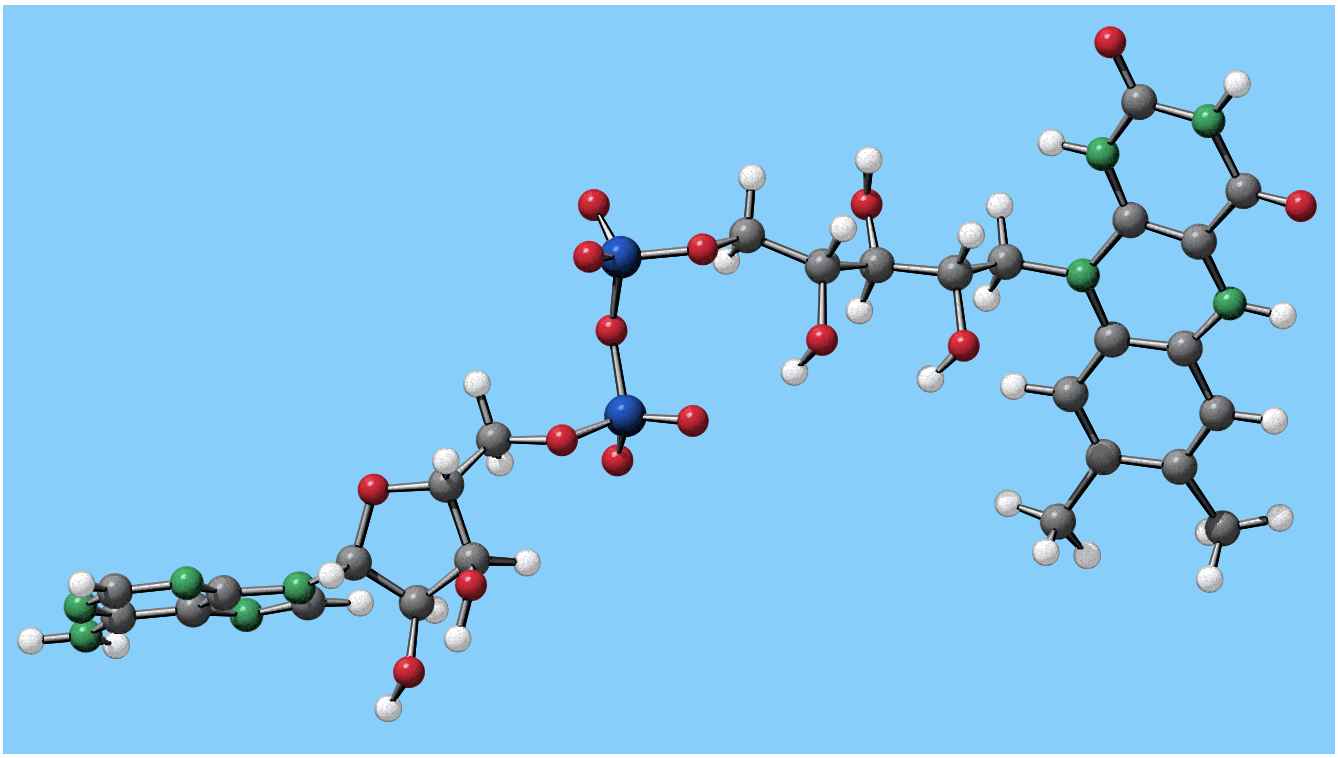

Figure 3 *One of the elongated I-shaped structures of $FADH_2$ as calculated with AMBER*

while after geometry optimization it is 51° for $FADH_2$ and 161° for $FADH^-$.

Apparently, differences in the intramolecular Coulomb interactions of FAD embodied in the force field parameters via differing partial charges, especially of the atoms in the heterocycle of the isoalloxazine moiety (see the section on computational details), result in noticeable conformational differences between $FADH^-$ and the fully reduced form $FADH_2$. This can also be seen for other structural characteristics, like the N1–N4 distance (6.9 and 8.1 Å for $FADH_2$ and $FADH^-$, respectively; see Table 1) or the dihedral angles C9A–N1–C4–C3 formed by atoms connecting the isoalloxazine and the sugar groups (86° and 44°, respectively). The most significant difference in properties between the two redox states of FAD is in the charge distribution; not unexpectedly, the negative charge of $FADH^-$ essentially resides on the pyrimidine moiety of isoalloxazine (i. e. predominantly on the carbonyl functions).

Another structural feature of FAD is the butterfly characteristic of the electron donor component isoalloxazine: both outermost rings of this moiety remain almost planar during all simulations while the interconnecting heterocycle is folded along the $N\cdots N_1$ axis (see Figure 1). Deviations from planarity can be quantified by the corresponding interplanar angle α which we define by the midpoint between N and N_1 and the centers of gravity of the two outermost rings. In order to emphasize the deviation from planarity we have chosen α = 0° to correspond to a coplanar conformation. In the crystal structure of the photolyase enzyme, the cofactor is slightly nonplanar with α = 3°.[1] The angle α is noticeably larger in the energy minimized structures of the isolated U-shaped systems: 8° and 28° for $FADH_2$ and $FADH^-$, respectively. These values are in accordance with quantum chemical calculations of reduced flavin models which show that isoalloxazine is folded by about 11–27° [37,38].

Simulation of FAD in water

To investigate environmental effects on the structure, FAD was embedded in a cluster of 585 water molecules. This solvent cluster is assumed to provide an adequate model for aqueous solution. MD simulations with subsequent geometry optimizations demonstrate the overall flexibility of the flavin molecule in solution as indicated by a large number of different conformations. As in the gase phase, the phosphate groups form the most flexible part of the molecule. The calculated conformations of FAD in aqueous solution are similar to those found for the isolated species. To support this statement we note that values for the N1–N4 distance range from about 6 to 15 Å. Furthermore, the butterfly characteristics of the isoalloxazine fragment can be clearly seen during the MD simulations: for $FADH_2$ the interplanar angle is 12° ± 8° while for $FADH^-$ the deviation from planarity is 20° ± 15°. Comparing these data to those from MD simulations on isolated molecules (α = 15° ± 6° and 24° ± 7° for $FADH_2$ and $FADH^-$, respectively) we note a slight propensity towards planarity.

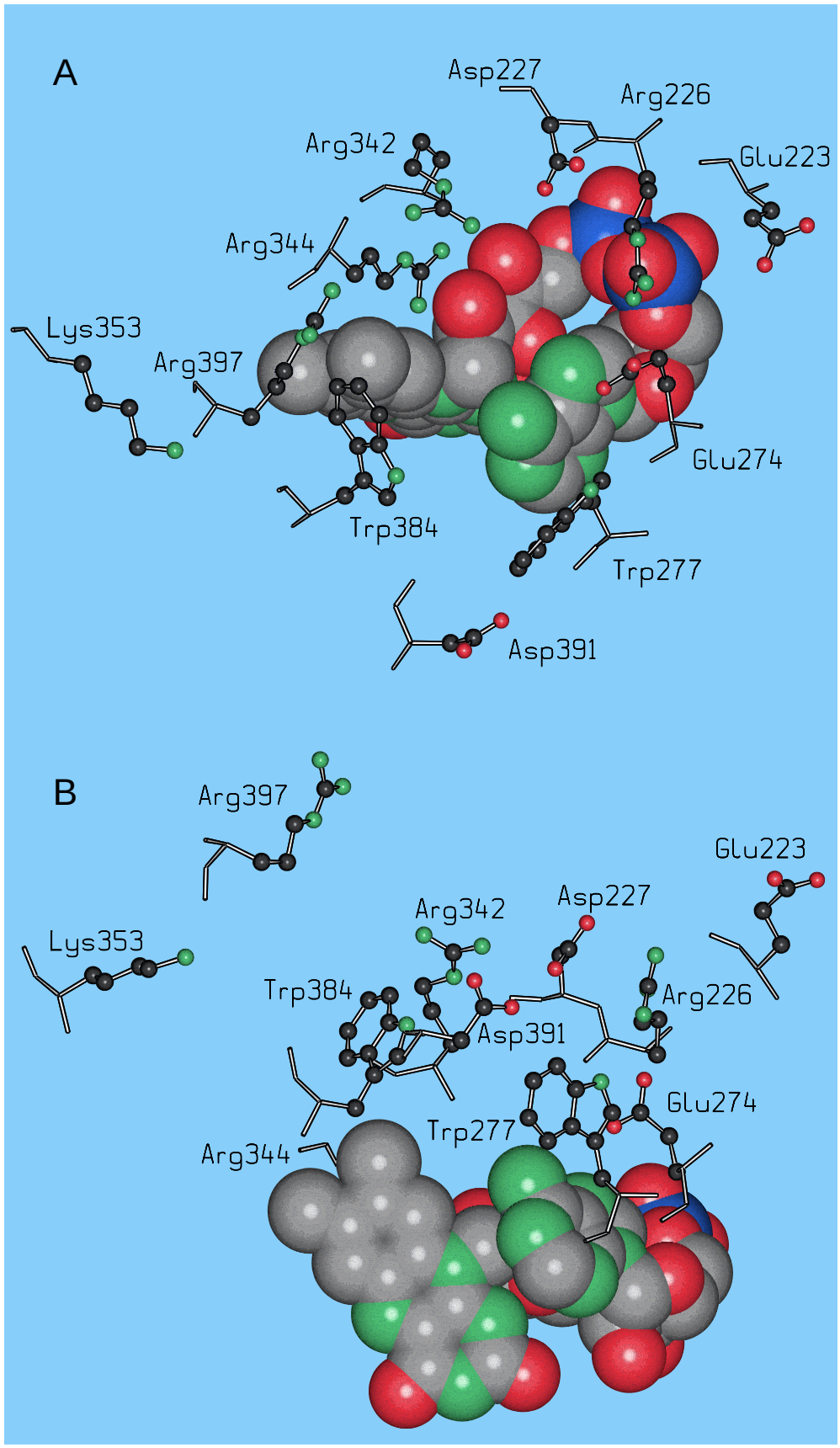

Figure 4 *FAD bound in the enzyme photolyase as determined in the X-ray crystal structure analysis of Ref. (1). Several amino acids adjacent to FAD in the enzyme pocket are also shown. Hydrogen atoms are omitted for clarity.* **A***: front view, looking through the pocket towards FAD located at the bottom of the cavity;* **B***: side view, the protein extends to the left and right of FAD as well as below FAD while the pocket is above. The pyrimidine like part of the isoalloxazine moiety is directed towards the interior of DNA photolyase*

A possible relaxation of solvated U-shaped FAD is of great interest and was therefore studied by energy minimization. As in case of the isolated species, optimization affects mostly the dihedral angle N1–C4–C3–C2 and the torsions around the P-O bonds (Table 1). However, the structures of isolated and solvated FAD molecules are in general rather similar. Furthermore, the differences between the structures of $FADH^-$ and $FADH_2$ in solvent correspond essentially to those already identified in the geometry optimization for the isolated molecules. Thus, one can conclude that the influence of an aqueous solvent on the structure of the flavin molecule is negligible. Nevertheless, two modest effects are worth mentioning. First, the N1–N4 distance is slightly reduced, from 6.9 to 6.5 Å for $FADH_2$ and from 8.1 to 7.8 Å for $FADH^-$ as compared to free FAD. Second, the interplanar angle also decreases from 8° to 3° for $FADH_2$ and from 28° to 10° for $FADH^-$. Both changes are such that solvation leads to closer similarity with the crystal structure where the N1–N4 distance is 5.9 Å and the interplanar angle $\alpha = 3°$ [1]. With these differences and similarities in mind one may state that the photolyase enzyme wraps the cofactor FAD without enforcing structural changes that entail an energy penalty.

In conclusion, no significant difference between isolated FAD and FAD in aqueous solution (modeled by a sphere filled with 585 solvent molecules) are found, irrespective of the redox state $FADH_2$ or $FADH^-$. Both derivatives are able to easily adopt the U-shaped conformation found in the crystal structure of the photolyase enzyme. Nevertheless, this form needs to be stabilized within the enzyme due to the immense flexibility of the flavin molecule. In the following, the structure of FAD as trapped in the enzyme will be discussed in the light of a molecular dynamics simulation of the enzyme DNA photolyase.

On the dynamics of FAD in photolyase

In the following we will discuss the results of the MD simulations performed on the system composed of (i) the photolyase enzyme, (ii) the cofactor FAD fitted into the pocket, and (iii) the water molecules filling up this pocket and solvating the enzyme. In the present section we focus on aspects directly connected to FAD, in the following section we shall address the enzyme environment.

Two important observations can be reported from the MD simulations. First, the flavin molecule stays bound to the enzyme, and second, in contrast to simulations of the isolated or water solvated flavin, the U-shaped conformation persists without significant changes, even after continuing the simulations up to 1.2 ns [39]. Therefore, due to the steric restrictions of the enzyme, the FAD molecule is almost inflexible and remains approximately in the crystal structure (see Table 1, Figures 2 and 4): the mean N1–N4 distance is about 6.0 Å with fluctuations of roughly 0.5 Å and an RMS value of 1.2 Å in the time window from 80 to 300 ps. The dihedral angles exhibit standard deviations of less than 13°, except for the phosphate groups which show deviations of up to 39°. However, these latter variations do not affect the overall FAD structure. Furthermore, no significant differences were found between the structures of $FADH^-$ and $FADH_2$.

When we compare these results to those from the geometry optimizations of the U-shaped form of isolated or water solvated FAD we note a tendency towards a smaller N1–N4 distance (Table 1). As mentioned above, this distance decreases slightly in going from the isolated flavin molecule to FAD in water. In the enzyme MD simulations the N1–N4 distance decreases even further towards the value found in the crystal structure, 5.9 Å. Especially for $FADH^-$, the photolyase enzyme brings both moieties, isoalloxazine and adenine, closer together, from 7.8 Å in solution to 6.1 Å in the enzyme simulation. Likewise, the isoalloxazine fragment is somewhat flattened (Table 1); during the MD run the conformation exhibits a slight deviation from planarity as measured by the interplanar angle α of 7° ± 5°. Above all, in case of $FADH^-$ the environment (the enzyme or the solvent) obviously reduces the mobility of the butterfly characteristics as compared to free FAD (Table 1). As expected, both $FADH^-$ and $FADH_2$ in their U-shaped conformation fit nicely into the pocket of the enzyme.

On the dynamics of the FAD environment in photolyase

As mentioned above, the flavin molecule remains bound to the enzyme pocket during the entire simulation. U-shaped FAD occupies the "bottom" of the enzyme cavity in such a way that the phosphate groups and the ribose moiety are more or less covered by the protein, while the other side, formed by isoalloxazine and adenine, is partially exposed to the substrate (see Figure 4). It is interesting to note that, in agreement with the X-ray structure analysis, implantation of FAD into the protein yields a structure where the pyrimidine part of the isoalloxazine group is directed to the interior of the enzyme; in particular, it is covered by the polar amino acids Asp372 and Arg344 which are mutually hydrogen bonded. For steric reasons, it is not expected that the orientation of the isoalloxazine moiety can be significantly changed.

Translating the asymmetry of the charge distribution of $FADH^-$ as calculated for the gas phase to the enzyme would imply that the negative charge density is directed towards the interior of the protein. Whether such a charge distribution holds also "in vivo" is not known as the present calculations do not account for the charge distribution in the electronically excited state $FADH^{-*}$ nor do they include any modification under the influence of the protein environment or the molecules in the binding pocket (water and substrate).

While the mean conformation of the chromophore as determined in the MD simulations is rather similar to the crystal structure, we note significant displacements of several amino acids. Two major regions in the crystal structure remain essentially unchanged during the MD simulations although individual amino acids are very mobile and some hydrogen bonds are formed and disrupted: (i) the hydrogen bonded network which covers the phosphate and ribose groups, and (ii) the hydrophobic shell in the neighborhood of the isoalloxazine and adenine units which, for example, con-

tains the following amino acids: Phe396, Phe399, Ala392, Ala393, Trp384, and Trp277 (Figure 4).

In the following, we shall discuss the hydrogen bonded network in greater detail. In the crystal structure one finds that the phosphate and parts of the ribose groups of FAD are shielded from direct access of the solvent or the substrate by polar amino acids, like Glu223 and Arg344; some of them are forming hydrogen bonds (Arg342 and Asp227 as well as Arg226 and Glu274; see Figure 4). Likewise, Arg344 forms a hydrogen bond with the negatively charged oxygen center O1 of FAD. The mentioned hydrogen bonds remain rather well established during the simulations, with the exception of that between Arg342 and Asp227. Moreover, in the course of the MD run the hydrogen bonds are complemented by new ones, e. g. between Arg342 or Arg226 and water molecules. Interestingly, due to the mobility of specific amino acids, rearrangements of the hydrogen bonds may occur. For example, during the MD simulation the glutamic acid Glu223 first shifts somewhat from its position in the crystal coordinates (by 1–2 Å, up to 100 ps) and afterwards departs considerably, by 4–5 Å. This enables Glu223 to move in between the two units Arg226 and Arg342 (Figure 4); each of these two amino acids is also displaced from its crystal location. After a shift by only about 2 Å Arg226 is able to form a hydrogen bond with Glu223 (after 60 ps). On top of that, Arg342 is displaced by about 7 Å from its location in the crystal and, after 80 ps, this arginine also forms a hydrogen bond with Glu223. On the other hand, Arg226 and Glu274 are less mobile, shifting only by about 2–3 Å from their location in the crystal; the hydrogen bond between them persists during the entire MD simulation. To summarize, while several amino acids and water molecules (both crystal water and solvent molecules) are very mobile during the simulation, the hydrogen bonded network remains more or less intact and shields to some extent the phosphate and ribose groups from the solvent.

The crystal and bulk water molecules fill up the pocket and solvate the enzyme. During the simulation the pocket of the enzyme which is assumed to accommodate the pyrimidine dimer [1] retains its overall shape to a large extent. This statement is supported by the observation that the number of solvent water molecules inside the pocket remains rather constant during the simulation. The number of water molecules inside the pocket has been estimated during the simulation. On the average about 19 water molecules are found within a distance of about 10 Å measured from center N1 of FAD towards the surface of the enzyme. This region roughly spans the depth of the pocket since center N1 resides at the "bottom" of the cavity. Within a distance of up to 15 Å from FAD, one counts on the average 59 water molecules.

Conclusions

The sensitivity of the conformational diversity of the FAD molecule with respect to its environment has been put to test in molecular dynamics simulations covering FAD (i) in the gas phase and in aqueous solution as well as (ii) in the enzyme DNA photolyase.

(i) In both the gas phase and aqueous solution, the FAD species under investigation, $FADH^-$ and $FADH_2$, turned out to be very flexible. A variety of conformations were found within an energy range of 8 kcal/mol; however, none of them is energetically preferred in a clear fashion. With regard to FAD as a cofactor of the enzyme photolyase, it is interesting to note that among the variety of conformations also U-shaped forms of FAD are encountered in the MD simulations.

(ii) The dynamics of FAD bound to photolyase is essentially governed by steric restrictions due to the enzyme. In contrast to FAD in the gas phase and in aqueous solution, and, last but not least, at variance with all known FAD binding proteins, the enzyme photolyase enforces a unique U-shaped conformation of FAD. Most probably, this U-shaped structure ensures a fixed geometry of the electron donor moiety isoalloxazine, a central functional feature of the photolyase. The calculated geometry of FAD is in very good agreement with the recent X-ray crystal structure analysis [1]. This conformation has also been shown to be independent of the redox state: the U-shaped structure is the same for $FADH_2$ and for the reduced species $FADH^-$ that is active in DNA repair. It is interesting to note that in $FADH^-$ the negative charge density on the isoalloxazine moiety is directed towards the interior of the protein. Unless this feature is significantly affected by either electronic excitation and/or the environment, the part of the cofactor $FADH^-$ active in electron transfer is not directly accessible to relevant molecules in the pocket, water solvent and substrate.

In the time window of 300 ps covered by the molecular dynamics of this investigation several important features persist: (i) the U-shaped conformation of FAD, (ii) the shape of the substrate docking site which is a pocket in the protein, (iii) the number of water molecules (19) residing inside the enzyme pocket, (iv) the network of hydrogen bonds involving amino acids and water which form the neighborhood of the phosphate and ribose groups of FAD, and (v) the hydrophobic shell covering essentially the isoalloxazine and adenine parts of the FAD. These structural features persist during the MD simulations although individual amino acids and water molecules are shown to be quite mobile.

Acknowledgments The authors thank Alexandr A. Voityuk and Serge Antonczak for fruitful discussions. This work has been supported by the Deutsche Forschungsgemeinschaft through SFB 377 and by the Fonds der Chemischen Industrie.

References

1. Park, H.-W.; Kim, S.-T.; Sancar, A.; Deisenhofer, J. *Science* **1995**, *268*, 1866.
2. Sancar, A. *Biochemistry* **1994**, *33*, 2.
3. Heelis, P. F.; Hartman, R. F.; Rose, S. D. *J. Photochem. Photobiol. A. Chem.* **1996**, *95*, 89.

4. (a) Voityuk, A. A.; Michel-Beyerle, M.-E.; Rösch, N. *J. Am. Chem. Soc*. **1996**, *118*, 9750. (b) Voityuk, A. A.; Rösch, N. *J. Phys. Chem. A* **1997**, *101*, 8335.
5. Djordjevic, S.; Pace, C. P.; Stankovich, M. T.; Kim, J. J. P. *Biochemistry* **1995**, *34*, 2163.
6. Hecht, H. J.; Kalisz, H. M.; Hendle, J.; Schmid, R. D.; Schomburg, D. *J. Mol. Biol.* **1993**, *229*, 153.
7. Mittl, P. R. E.; Schulz, G. E. *Protein Sci.* **1994**, *3*, 799.
8. Karplus, P. A.; Schulz, G. E. *J. Mol. Biol.* **1989**, *210*, 163.
9. Gatti, D. L.; Entsch, B.; Ballou, D. P.; Ludwig, M. L. *Biochemistry* **1995**, *35*, 567.
10. Mattevi, A.; Obmolova, G.; Kalk, K. H.; van Berkel, W. J. H.; Hol, W. G. J. *J. Mol. Biol.* **1993**, *230*, 1200.
11. Mattevi, A.; Obmolova, G.; Sokatch, J. R.; Betzel, C.; Hol, W. G. J. *Proteins Struct. Funct.* **1992**, *13*, 336.
12. Lantwin, C. B.; Schlichting, I.; Kabsch, W.; Pai, E. F.; Krauth-Siegel, R. L. *Proteins Struct. Funct.* **1994**, *18*, 161.
13. Stehle, T.; Ahmed, S. A.; Claiborne, A.; Schulz, G. E. *J. Mol. Biol.* **1991**, *221*, 1325.
14. Schreuder, H. A.; Prick, P. A. J.; Wierenga, R. K.; Vriend, G.; Wilson, K. S.; Hol, W. G. J.; Drenth, J. *J. Mol. Biol.* **1989**, *208*, 679.
15. Schreuder, H. A.; van der Laan, J. M.; Hol, W. G. J.; Drenth, J. *J. Mol. Biol.* **1988**, *199*, 637.
16. Lah, M. S.; Palfey, B. A.; Schreuder, H. A.; Ludwig, M. L. *Biochemistry* **1994**, *33*, 1555.
17. Waksman, G.; Krishna, T. S. R.; Williams, C. H. J.; Kuriyan, J. *J. Mol. Biol.* **1994**, *236*, 800.
18. Kuriyan, J.; Krishna, T. S. R.; Wong, L.; Guenther, B.; Pahler, A.; Williams, C. H. J.; Model, P. *Nature* **1991**, *352*, 172.
19. Bailey, S.; Smith, K.; Fairlamb, A. H.; Hunter, W. N. *Eur. J. Biochem.* **1993**, *213*, 67.
20. Bailey, S.; Smith, K.; Fairlamb, A. H.; Hunter, W. N. *Acta Cryst. D.* **1994**, *50*, 139.
21. Stehle, T.; Claiborne, A.; Schulz, G. E. *Eur. J. Biochem.* **1993**, *211*, 221.
22. Kuriyan, J.; Kong, X. P.; Krishna, T. S. R.; Sweet, R. M.; Murgolo, N. J.; Field, H.; Cerami, A.; Henderson, G. B. *Proc. Nat. Acad. Sci. USA* **1991**, *88*, 8764.
23. Karplus, P. A.; Schulz, G. E. *J. Mol. Biol.* **1987**, *195*, 701.
24. Mattevi, A.; Schierbeek, A. J.; Hol, W. G. J. *J. Mol. Biol.* **1991**, *220*, 975.
25. Kim, J.-J. P.; Wang, M.; Paschke, R. *Proc. Nat. Acad. Sci. USA* **1993**, *90*, 7523.
26. Watt, W.; Tulinsky, A.; Swenson, R. P.; Watenpaugh, K. O. *J. Mol. Biol.* **1991**, *218*, 195.
27. Weiner, S. J.; Kollmann, P. A.; Case, D. A.; Singh, U. C.; Ghio, C.; Alagona, G.; Profeta, S. J.; Weiner, P. *J. Am. Chem. Soc.* **1984**, *106*, 765.
28. Weiner, S. J.; Kollmann, P. A.; Nguyen, D. T.; Case, D. A. *J. Comp. Chem.* **1986**, *7*, 230.
29. *Discover User Guide*, October 1995. San Diego: Biosym/ MSI, 1995.
30. Stewart, J. J. P. *MOPAC 6.0*, Quantum Chemistry Program Exchange no. 455.
31. Stewart, J. J. P. *J. Comp. Chem.* **1989**, *10*, 209, 221.
32. Greengard, L.; Rokhlin, V. I. *J. Comp. Phys.* **1987**, *73*, 325.
33. Schmidt, K. E.; Lee, M. A. *J. Stat. Phys.* **1991**, *63*, 1223.
34. Ding, H. Q.; Karasawa, N.; Goddard, W. A. *J. Chem. Phys.* **1992**, *97*, 4309.
35. Press, W. H.; Teukolsky, S. A.; Vetterling, W. T.; Flannery, B. P. *Numerical Receipes* 2nd ed., Cambridge University Press, Cambridge, 1992.
36. Keller, E. *Program Schakal96*, Kristallographisches Institut der Universität Freiburg, Germany, 1996.
37. Meyer, M.; Hartwig, H.; Schomburg, D. *J. Mol. Struct. (Theochem)* **1996**, *364*, 139.
38. Hall, L. H.; Bowers, M. L.; Durfor, C. N. *Biochemistry* **1987**, *26*, 7401.
39. Hahn, J.; Michel-Beyerle, M.-E.; Rösch, N. to be published.